International Science and Technology Journal
المجلة الدولية للعلوم والتقنية
Volume 37 العدد
Part 2 المجلد
ISTJ

http://www.doi.org/10.62341/ahly2841

Received	**2025/10/30**	**تم استلام الورقة العلمية في**
Accepted	**2025/11/25**	**تم قبول الورقة العلمية في**
Published	**2025/11/26**	**تم نشر الورقة العلمية في**

Investigation of Adsorption Isotherms, Kinetics, and Thermodynamics of Copper and Lead Removal by Zirconium Phosphate

Abubaker Abutartour [1], Huda Ben Ighwaylah[1], Lotfia El Majdoub[2], Yaseen Elhebshi[3], Nader Elaziby[1]

1. Libyan Advanced Center for Chemical Analysis, Libyan Authority for Scientific Research - Libya
2. University of Tripoli, Faculty of Science - Libya
3. University of Gharyan, Faculty of Science - Libya

*Corresponding author: abobaker.abase8@aal.ly.com

Abstract

This research focuses on the elimination of copper and lead ions from water using zirconium phosphate as an adsorbent. Building upon previous work focused on adsorption isotherms and kinetic models, the adsorption behavior was evaluated using models done by (Lang, Freu, Tem, and Dub–Radus). The findings indicated that the Freu model was the most precise in representing copper ion adsorption, suggesting that the adsorption occurs on a heterogeneous surface (R^2 = 0.984). In contrast, the Langmuir model provided the best description for the adsorption of lead ions, aligning with the concept of monolayer adsorption on a uniform surface (R^2 = 0.923). Kinetic studies indicated that intra-particle diffusion played a crucial role in the adsorption process. The findings showed that the process was endothermic and spontaneous. The positive $\Delta S°$ value implies an increase in disorder at the solid-liquid interface. Overall, zirconium phosphate displayed significant potential as an effective adsorbent for the removal of Pb(II) and Cu(II) ions from water, providing useful information for enhancing adsorption-based water treatment systems.

Key Words: Zirconium phosphate, Adsorption isotherms, Lead Adsorption, Isotherm models.

International Science and Technology Journal
المجلة الدولية للعلوم والتقنية
Volume 37 العدد
Part 2 المجلد
http://www.doi.org/10.62341/ahly2841

دراسة نظريات الامتزاز والحركيات والديناميكا الحرارية لإزالة النحاس والرصاص باستخدام فوسفات الزركونيوم

أبو بكر أبو طرطور[1]، هدى بن إغويلة[1]، لطفية المجدوب[2]، ياسين الحبشي[3]، نادر العزيبي[1]

1. المركز الليبي المتقدم للتحاليل الكيميائية، الهيئة الليبية للبحث العلمي، ليبيا
2. كلية العلوم – جامعة طرابلس، ليبيا
3. كلية العلوم – جامعة غريان، ليبيا

الملخص:

تُعدّ مشكلة تلوث المياه بالمعادن الثقيلة مثل النحاس مثل النحاس والرصاص من أبرز القضايا البيئية التي تهدد صحة الإنسان واستدامة النظم البيئية، الأمر الذي يستدعي طوير مواد فعّالة لمعالجة هذه الملوثات. في هذه الدراسة تم استخدام فوسفات الزركونيوم كمادة ماصّة لإزالة أيونات النحاس والرصاص من المحاليل المائية، حيث تم تحليل سلوك الامتزاز بالاعتماد على نماذج الامتزاز المعروفة وهي: لانكماير وفريندلخ وتيمكن ودوبينين– رادوشكيفيتش، أظهرت النتائج أن نموذج فريندلخ هو الأنسب لوصف امتزاز أيونات النحاس مما يشير إلى حدوث الامتزاز على سطح غير متجانس، بينما كان نموذج لانكماير الأكثر ملاءمة لامتزاز أيونات الرصاص وهو ما يدل على امتزاز أحادي الطبقة على سطح متجانس. كما بينت التحليلات الحركية أن الانتشار داخل الجزيئات يلعب دوراً مهماً في عملية الامتزاز، وأظهرت الحسابات الثرموديناميكية أن العملية ماصّة للحرارة وعفوية بطبيعتها، مع زيادة في العشوائية عند واجهة الصلب–السائل. توصي هذه الدراسة بإجراء مزيد من الأبحاث لتطوير وتحسين خصائص فوسفات الزركونيوم كمادة ماصّة فعالة لإزالة المعادن الثقيلة وتعزيز تطبيقها في أنظمة معالجة المياه .

الكلمات المفتاحية: فوسفات الزركونيوم، نظريات الامتزاز، امتزاز الرصاص، نماذج الامتزاز

1. Introduction

Adsorption and separation represent an important application for hybrid porous materials [1–4]. Recent studies have concentrated on

http://www.doi.org/10.62341/ahly2841

developing various porous organic-inorganic hybrid materials aimed at effectively extracting heavy metal ions, especially cadmium (Cd^{2+}), copper (Cu^{2+}), and lead (Pb^{2+}), from polluted wastewater [5,6]. The integration of organic functional groups into porous systems is a key design strategy for enabling effective metal ion coordination and sequestration [7]. Specific functional motifs, including thiol, thiourea, and amine groups, have been strategically incorporated into mesoporous silica and titanium phosphonate matrices to create effective binding sites for the selective extraction of Hg^{2+}, Cu^{2+}, and Cd^{2+} ions [8-11]. The initial isolation of C–P compounds from biological matrices by Horiguchi and Kandatsu over five decades ago paved the way for the broad utility of phosphinic acid in diverse applications [12]. The facile substitution of the hydroxyl group in phosphoric acid serves as a key synthetic step for generating a diverse array of phosphinic acids with tailored functional groups [13, 14]. The introduction of organic functional groups into metal phosphates via P–OH bond substitution results in significant structural distortion. This distortion subsequently perturbs the electron cloud density localized around the phosphorus atoms within the framework. Phosphonic acid is a versatile precursor for constructing open frameworks, the material's functionality is achieved due to its unique combination of inorganic oxide moieties and organic functional groups. The capability to incorporate a wide range of organic moieties provides a direct pathway for engineering materials with tunable structural properties. These open-framework metal phosphates, which occupy a structural niche between zeolites and organic metals, are versatile inorganic-organic hybrids. Their unique architecture makes them suitable for diverse applications, encompassing insertion reactions, ionic conduction, catalyzing reactions and exchanging ions [15,16]. Recent studies support this potential. For example, nano-crystalline ZrP has demonstrated impressive adsorption capacity and selectivity for heavy metal ions, Moreover, hybrid materials, where zirconium phosphate is functionalized with organic ligands or metal-oxide domains, have shown improved performance in removing Pb^{2+} and Cu^{2+} ions [17]. Building upon our 2014 findings, which demonstrated the efficacy of a hierarchical porous zirconium phosphate membrane in adsorbing Cu(II) and Pb(II) ions [17], this work aims to significantly broaden the scope of that investigation.

http://www.doi.org/10.62341/ahly2841

The previous study underscored the critical role of the material's bimodal macro-mesoporous network and its -Si-O- linkages in facilitating metal ion binding and transport. The aim of this research is to elucidate the sequestration mechanisms of Cu(II) and Pb(II) ions on zirconium phosphate. To this end, the equilibrium and kinetic data are rigorously analyzed using a suite of models, including the Lang, Freu, Tem, and Dub–Radus isotherms, as well as pseudo first and second order, and inside-particle dissemination kinetics. This systematic approach provides deeper mechanistic insights into the adsorption process and allows for assessing zirconium phosphate's efficiency and potential for practical water treatment applications.

2. Experiments

2.1. Materials

Zirconium dichloride oxide octahydrate ($ZrOCl_2 \cdot 8H_2O$) and Bis(hexamethylenetriaminepenta (methylenephosphonic acid)) (BMTPA) were obtained from Sinopharm Chemical Reagent Co. (China). Silicon tetrafluoride (SiF_4) and hexadecyl trimethyl ammonium bromide (CTAB) were acquired from Beijing Chemical Reagent Co. (China).

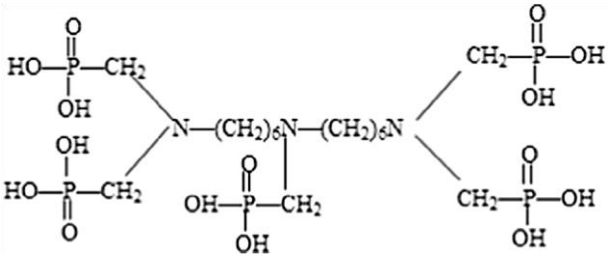

Scheme 1. Structural formula of BMTPA.

2.2. Synthesis of the Porous Adsorbent (BHAZP)

The synthesis commenced with the preparation of separate aqueous solutions of 0.30 M $ZrOCl_2$ (with added SiF_4) and 0.60 M BMTPA. The $ZrOCl_2/SiF_4$ solution was added dropwise into the BMTPA solution under a nitrogen atmosphere with vigorous stirring, immediately generating a white suspension. This suspension was subsequently refluxed at 80 °C for 2 h, followed by hydrothermal treatment in a Teflon-lined autoclave at 80 °C for 24 h. The product

http://www.doi.org/10.62341/ahly2841

was isolated by centrifugation, repeatedly washed with deionized water then dried at 70 °C. The final porous framework was obtained ethanol was used to remove surfactant by reflux for one day.

2.3. Batch Adsorption Experiments

The adsorption of copper and lead ions was evaluated via batch experiments. Specifically, 0.10 g of BHAZP adsorbent was introduced into 100 mL of metal ion solution (50–900 ppm) contained in a 250 mL glass bottle. The suspension was agitated at room temperature for one day to achieve equilibrium sorption capacity. Subsequently, the supernatant was analyzed by atomic absorption spectroscopy to determine the residual metal concentration. The equilibrium adsorption, p_e (mg g^{-1}), was determined as follows [16]:

$$\mathbf{p_e = (E_0 - E_e)\ V / m}$$

Where:

$\mathbf{E_0}$ and $\mathbf{E_e}$ are initial and equilibrium liquid-phase concentrations of metal ions (mg L^{-1}),

V is volume of the solution (L), and **m** is the mass of the dry adsorbent (g).

3. Results and discussion

3.1. Isotherm data analysis

Adsorption isotherm analysis provides critical insights into the interactions between the sorbent and sorbate. The equilibrium data were modeled using the Lang, Freu, Tem, and Dub–Radus isotherm models to characterize the uptake of metal ions. The Lang isotherm model, originally developed for gas-phase adsorption on solids, is widely applied to describe monolayer adsorption at the solid-liquid interface. It presupposes a homogeneous adsorbent surface with identical, energetically equivalent sites, where adsorption occurs in a single layer without intermolecular interactions. The model describes a dynamic equilibrium between adsorption and desorption processes. Its linearized form is commonly expressed as follows:

$$\frac{\mathbf{1}}{\mathbf{Pe}} = \frac{\mathbf{1}}{\mathbf{P}\boldsymbol{max}\ \mathbf{kl}}\ \frac{\mathbf{1}}{\mathbf{ce}} + \frac{\mathbf{1}}{\mathbf{P}\boldsymbol{max}} \qquad (\mathbf{1})$$

http://www.doi.org/10.62341/ahly2841

In the equations, pmax (mg/g) indicates the highest capacity for adsorption, while kl (L/mg) is a constant that is indirectly associated with the energy of adsorption and illustrates the attraction between the adsorbate and adsorbent. The parameters Pmax and kl can be obtained from Equation (1) through the slope derived from the linear graph of 1/Pe versus 1/ce. Additionally, the dimensionless equilibrium parameter RL can indicate whether the isotherm is favorable, unfavorable, irreversible, or linear, depending on whether RL is less than 1, greater than 1, equal to 0, or equal to 1, respectively [2]. This is expressed by Equation (2) as follows:

$$\boldsymbol{Rl} = \frac{\mathbf{1}}{(\mathbf{1}+\boldsymbol{klCi})} \qquad (\mathbf{2})$$

Where: C_i = initial concentration KL
The Freu model is an appropriate formula which can be applied to multiphase systems, involving interactions between the adsorbed molecules. It is possible to determine if the adsorption is linear (n = 1), a chemical process (n < 1), or a favorable physicochemical phenomenon (n> 1) using the n parameter, also referred to as the heterogeneity factor [3]. The Freu model can be expressed as Equation (3):

$$\mathbf{\log Pe} = \frac{\mathbf{1}}{\mathbf{n}} \ \mathbf{\log Ce} + \mathbf{\log Kf} \qquad (\mathbf{3})$$

Where:
$\mathbf{P_e}$ amount of metal ion adsorbed (mg g^{-1}). $\mathbf{C_e}$ equilibrium concentration (mg L^{-1}).
Kf Freu constant. **n** Freu exponent related to adsorption intensity and surface heterogeneity.
The Tem isotherm was developed on the premise that the heat of adsorption of all molecules within the layer follows a linear relationship rather than a logarithmic one, as suggested by the Freu equation. This model is applicable solely in a moderate range of ion concentrations [4]. The Tem isotherm can be expressed by Equation (4).

$$\mathbf{P_e} \ = \ \mathbf{B \ln A_T} \ + \ \mathbf{B \ln C_e} \qquad (\mathbf{4})$$

http://www.doi.org/10.62341/ahly2841

Where, B = RT/ b [constant related to heat of sorption (J/mol) obtained from the Tem plot (P_e versus lnC_e)], AT = Tem isotherm equilibrium binding constant (L/g);
b = Tem constant-temperature curve; R = ideal gas constant (8.314 $J \cdot mol^{-1} \cdot K^{-1}$)
T = Temperature at 298 °C.
The Dub–Radus isotherm is employed to determine the apparent adsorption energy and characterize the adsorption process type [5]. The linearized form of this model is expressed by the following equation:

$$\ln P_e = \ln P_m - \beta\varepsilon^2 \qquad (5)$$

Where:
P_e amount of adsorbed metal ions (mg/g), P_m maximum adsorption capacity (mg/g),
β is the D-R constant related to the mean adsorption energy (mol^2/kJ^2),
ε is the Polanyi potential, R ideal gas constant (8.314 J/mol·K),
T absolute temp (K), C_e is the equilibrium concentration of metal ions in solution (mg/L).
The apparent adsorption energy can be derived by constant of β using the relationship as in equation 6:

$$E = \frac{1}{\sqrt{2\beta}} \qquad (6)$$

This energy value helps distinguish between physisorption and chemical adsorption. The magnitude of the apparent adsorption energy (E) characterizes the nature of the adsorption process. An E value ranging from 8 to 16 kJ mol^{-1} signifies a chemisorption mechanism, such as ion exchange or surface complexation. Conversely, an E value less than 8 kJ mol^{-1} corresponds to physical adsorption. The equilibrium data fitted to these models are illustrated in Figure 1.

http://www.doi.org/10.62341/ahly2841

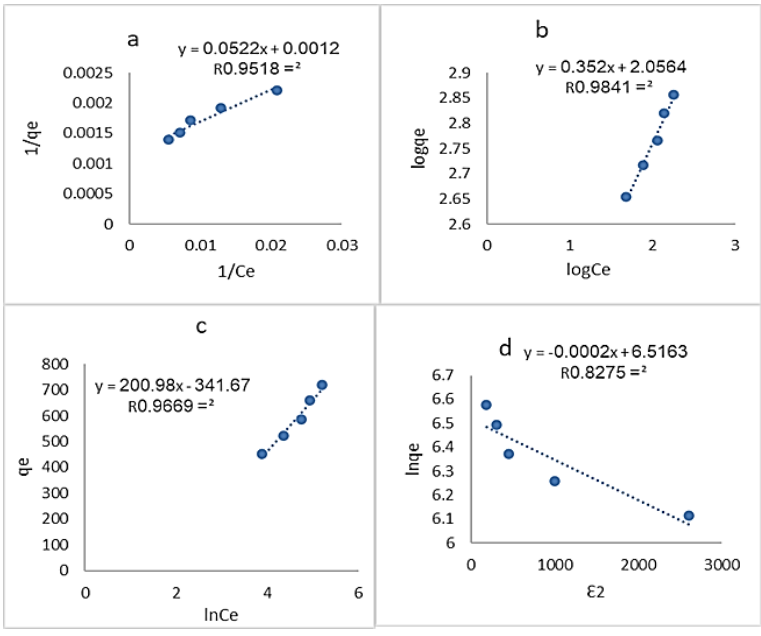

Figure (1) Isotherm Models for Adsorption of Cu (a) Lang (b) Freu (c) Tem (d) D-R

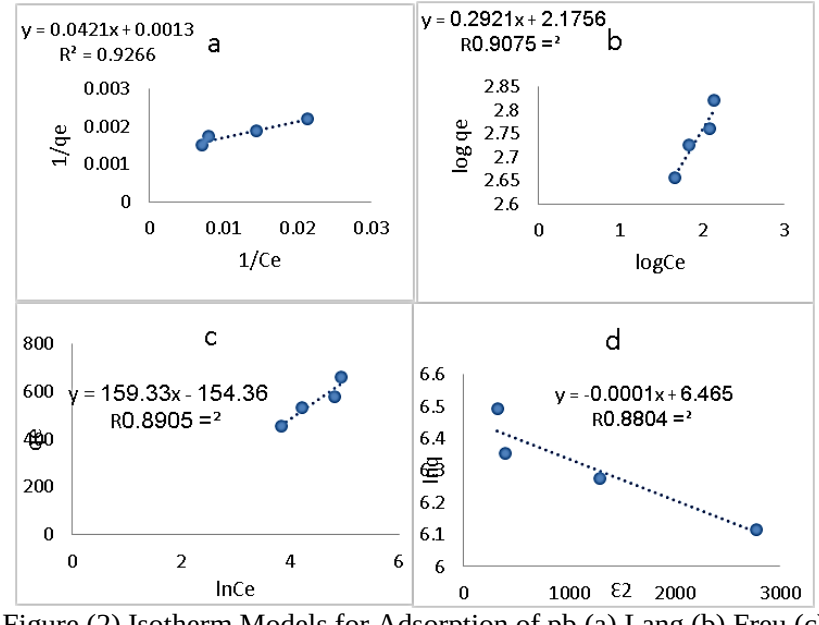

Figure (2) Isotherm Models for Adsorption of pb (a) Lang (b) Freu (c) Tem (d) D-R

http://www.doi.org/10.62341/ahly2841

3.2 Error Analysis

The optimal isotherm model can be identified by analyzing the correlation coefficient (R2). Despite its efficiency, this indicator can only solve isotherm models with linear forms.[6] Consequently, two distinct error functions were to determine the best isotherm model (SAE) and (ARE). For higher concentrations, the sum of absolute errors (SAE) (Equation (7)) likewise provides precise and accurate corrections. This occurs due to a higher error rate associated with a broader concentration range. The purpose of the average relative error (ARE) function (Equation (8)) is to minimize the distribution of fractional errors across the entire concentration spectrum.

$$SAE = \sum_1^n \left| q_{cal} - q_{exp} \right| \quad (7)$$

$$ARE = \frac{100}{n} \sum_1^n \left| \frac{q_{cal} - q_{exp}}{q_{exp}} \right| \quad (8)$$

for displaying the results of the experiment.

Table (1) Lang, Freu, Tem and Dub–Rad isotherm constants and correlation coefficients

Ion	Lang			Freu			Tem			Dub- Radu		
	P_{max} (mg/g)	Kl (L/mg)	R^2	KF (mg/g)	n	R^2	At	b	R^2	q_{max} (mg/g)	E (kJ mol^{-1})	R^2
Cu^{2+}	833.33	0.023	0.952	113.87	2.84	0.984	0.183	12.33	0.967	708.4	50	0.828
Pb^{2+}	769.23	.031	0.923	149.8	3.42	0.908	2.635	15.55	0.891	642.26	70.7	.88

Table 2: Error Analysis Values for Adsorption Isotherm Models

Ion	Lang		Freu		Tem		Dub- Radu	
	SAE	ARE	SAE	ARE	SAE	ARE	SAE	ARE
Cu^{2+}	119.58	3.89	54.60	1.857	79.75	2.79	206.83	7.18
Pb	80.60	3.32	87.71	3.77	83.56	3.55	146.78	6.66

Table 1 summarizes the maximum adsorption capacity (q_m), correlation coefficients (R^2), and associated parameters derived from the applied isotherm models. The results indicate that for cu, the experimental data was fitted to the Freu isotherm model with R^2 = 0.984 and qm = 445.36 mg/g; the experimental qe was 451.9 mg/g,

http://www.doi.org/10.62341/ahly2841

n = 2.84, and Kf = 113.87. This data shows that adsorption takes place on a non-uniform surface and follows a nonlinear distribution with n > 1. The high value of Kf indicates that the adsorbent has good adsorption capacity. To further confirm the model's suitability, error indices were calculated for each model from Table 2. The Freundlich model yielded the lowest values for both SAE (54.60) and ARE (1.857), thereby enhancing the model's reliability in representing a comparison of the experimental data with the other models. For pb, the Langmuir isotherm plot fitted the experimental data with R^2 = 0.927 and qm = 769.23 mg/g. Based on this data, we can conclude that adsorption occurs on a homogeneous surface and is a monolayer surface. To further confirm the model's suitability, error indices were calculated for each model from Table 2. The Langmuir model yielded the lowest values for both SAE (80.60) and ARE (3.32), thereby enhancing the model's reliability in representing a comparison of the experimental data with the other models.

3.3 Kinetic analysis:

The pseudo-first order, pseudo-second order and Intra-Particle Diffusion Model models are commonly used methods for describing adsorption kinetics. models assume that the rate of adsorption is directly related to the number of vacant sites available on the adsorbent. This can be expressed mathematically by the equation (9):

$$log(q_e - q_t) = \log q_e + K_1 \frac{t}{2.303} \quad (9)$$

Where k1 = the constant rate for the pseudo-first-order equation (min^{-1}) and qe = the amount of adsorbed dye at steady-state ($g \cdot mg^{-1}$). A linear relationship was obtained by plotting Log (qe-qt) against t.

3.3.1 Pseudo-Second-Order Model

The pseudo-second-order model indicates that the speed of adsorption is related to the square of the number of available sites. The linear representation of the pseudo-second-order model can be stated as Equation (10):

$$\frac{t}{qt} = \frac{1}{k2q_e^2} + \frac{t}{qe} \quad (10)$$

http://www.doi.org/10.62341/ahly2841

Where k_2 represents the pseudo-second-order rate constant for adsorption ($g \cdot mg^{-1} \cdot min^{-1}$). The values of q_e and k_2 can be obtained from the slope and intercept, respectively, of the linear graph plotting t/q_t against t. [8]

3.3.2 Intra-particle Diffusion Model

The intra-particle diffusion model is commonly utilized to explore the rate-limiting steps involved in the adsorption process, particularly when diffusion within pores plays a substantial role. This model suggests that the transport of adsorbate molecules into the internal pores of the adsorbent is a key element affecting the overall adsorption rate. As stated by Weber and Morris, the intra-particle diffusion model is represented as:

$$q_t = k_d\, t^{0.5} + C_i \qquad (11)$$

Were, kd the intra-particle diffusion rate constant (mg/g min), Ci constant. The value of Ci provides a quantitative measure of the boundary layer thickness. Figure 3 presents the kinetic model for the adsorption process. Figures 3.and 4 shows agreement between the experimental values and the theoretical model, the parameters of kinetic models of both cu and pb are summarized in table 3.

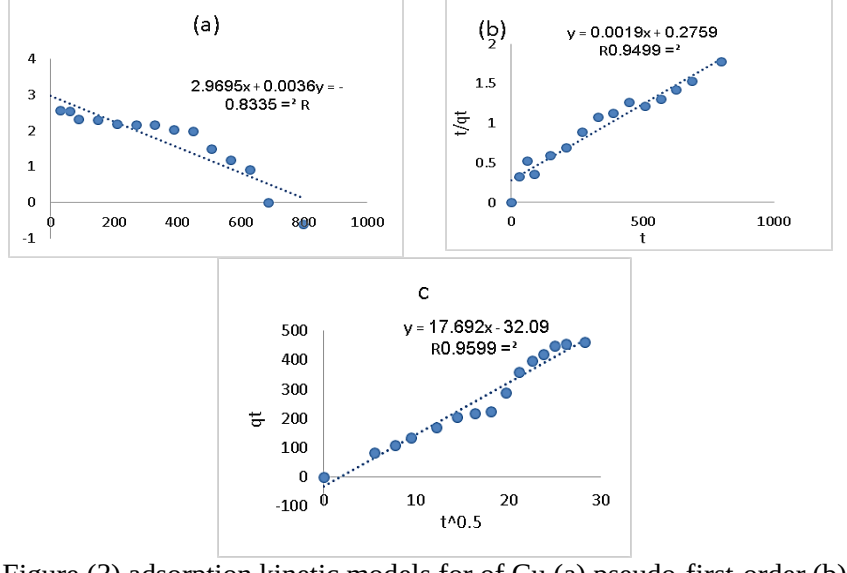

Figure (3) adsorption kinetic models for of Cu (a) pseudo-first-order (b) pseudo-second model. (c) intraparticle diffusion kinetic model

http://www.doi.org/10.62341/ahly2841

Table 3. Parameters of kinetic models for adsorption of cu and pb.

		pseudo-first-order			pseudo-second model			intraparticle diffusion kinetic model.		
cu	$q_e(exp)$ (mgg^{-1})	$K_1(min^{-1})$	q_e (mgg^{-1})	R^2	$K_2(min^{-1})$	q_e (mgg^{-1})	R2	$K_d(min^{-1})$	Ci	R2
	451.9	0.0067	903.65	0.83	5.83×10^{-6}	588.24	0.9499	17.69	18.54	0.96
pb	853.48	0.003	58.3	0.85	1.57×10^{-5}	909.09	0.94	32.09	49.66	0.95

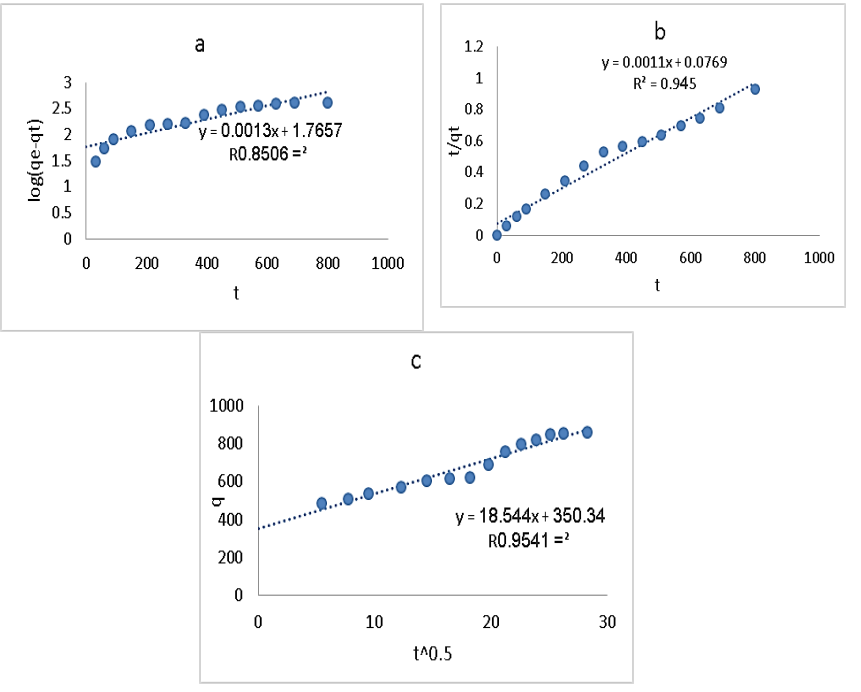

Figure (4) adsorption kinetic models for of pb (a) pseudo-first-order (b) pseudo-second model. (c) intraparticle diffusion kinetic model

3.4 Adsorption Thermodynamics

To evaluate the adsorption thermodynamics of cu and pb onto the adsorbent,equation (12) is commonly used [10]:

$$\Delta G^\circ = \Delta H^\circ - T\Delta S^\circ \qquad (12)$$

The spontaneity and nature of the sorption process were evaluated by determining the thermodynamic parameters: the change in Gibbs

http://www.doi.org/10.62341/ahly2841

free energy (ΔG°), enthalpy (ΔH°), and entropy (ΔS°). These values were derived from Equations (13) and (14):

$$\Delta G^\circ = -RT \ln Kd \quad (13)$$

$$\ln kd = \frac{(\Delta S^\circ)}{R} - \frac{(\Delta H^\circ)}{RT} \quad (14)$$

In this context, Kd represents the distribution coefficient, R denotes the universal gas constant, and T stands for the temperature in Kelvin measured on an absolute scale. The values for ΔHo and ΔSo were determined from the slopes and intercepts of a linear plot of lnKd against 1/T, while ΔHo was obtained using equation (14). The resulting thermodynamic parameters (ΔG°, ΔH°, and ΔS°) are summarized in Table 4.

Table 4. Thermodynamic Parameters for the Adsorption of Cu(II) and Pb(II) Ions

	Cu			Pb		
T (K°)	ΔG(KJ/mol	ΔH(KJ/mol)	ΔS(KJ/mol)	ΔG(KJ/mol)	ΔH(KJ/mol)	ΔS(KJ/mol)
297	1.188	34.75	- 0.117	0.302	46.35	0.151
303	1.585			-0.900		
313	3.577			-2.744		

The combined kinetic and thermodynamic results indicate that the pseudo-second-order model best describes the adsorption process of both Cu^{2+} and Pb^{2+} ions, indicating that the adsorption rate is controlled by the availability of surface active sites. However, the relatively low values of enthalpy (ΔH = 34.75 kJ/mol for Cu and 46.35 kJ/mol for Pb) reveal that the adsorption process is primarily physical in nature, as enthalpy values below approximately 40–50 kJ/mol typically correspond to weak interactions such as Van der Waals forces or electrostatic attractions, rather than strong chemical bonding. The endothermic nature of the adsorption process, confirmed by the positive ΔH° values, explains its enhanced favorability at elevated temperatures, Furthermore, the negative values of Gibbs free energy (ΔG) at elevated temperatures confirm the spontaneous nature of the adsorption process under these conditions. Therefore, it can be concluded that the overall adsorption mechanism occurs mainly through physisorption controlled by surface interactions and intraparticle diffusion, with a

http://www.doi.org/10.62341/ahly2841

minor contribution from chemisorption phenomena that stabilize the metal ions on the adsorbent surface. The positive intercept (14.163) produces an entropy change (ΔS°) of +117.79 J/mol K, indicating increased randomness at the solid-solution interface during adsorption, likely due to the rearrangement of the adsorbate molecules on the surface. The Gibbs free energy change (ΔG°) was calculated to be negative, indicating that the adsorption process is spontaneous under ambient conditions. Although ΔG° is negative, the relatively low magnitude, combined with a ΔH° value close to the boundary between physical adsorption and chemisorption, suggests that the process is likely physical adsorption with a small portion of chemisorption, where weak van der Waals forces dominate rather than chemical bond formation.

4. Conclusion

The adsorption behavior was comprehensively investigated using several isotherm models. The analysis revealed that copper adsorption followed the Freu model, indicating multilayer adsorption on a heterogeneous surface. In contrast, lead adsorption aligned more closely with the Lang model, suggesting monolayer coverage on a homogeneous surface. Kinetic studies demonstrated that intra-particle diffusion served as the primary rate-controlling mechanism, indicating favorable adsorption kinetics. Thermodynamic analysis confirmed that the adsorption processes were spontaneous and endothermic, with positive entropy change ($\Delta S^\circ > 0$) reflects an increase in disorder or randomness at the solid-liquid interface upon adsorption. The moderate enthalpy values suggest that physical adsorption mechanisms predominated, with some contribution from chemical interactions. Thus, the adsorption process involves a combination of both physisorption and chemisorption mechanisms. In summary, this study validates zirconium phosphate as a highly effective adsorbent for removing heavy metals from aqueous solutions. Future research should focus on optimizing operational parameters, scaling up for industrial applications, and evaluating the regeneration potential and reusability of the adsorbent to enhance its practical implementation.

http://www.doi.org/10.62341/ahly2841

5. References

[1] Chongdar S., S. Bhattacharjee, P. Bhanja, et al. Chemical Communications. (2022), 58, 3429
[2] Antochshuk V., and M. Jaroniec. Chem. Commun. (2002) 258–259 .
[3] Qiao S. Z., H. Djojoputro, Q. Hu, et al. Solid State Chem. 34 (2006) 249–256
[4] Vinu A., V. Murugesan, and M. Hartmann. J. Phys. Chem. B 108 (2004) 7323–7330
[5] Dai S., M. C. Burleigh, Y. S. Shin, et al. Angew. Chem. Int. Ed. 38 (1999) 1235–1239 .
[6] Liu A. M., K. Hidajat, S. Kawi, et al. Chem. Commun. (2000) 1145–1146
[7] Schroden R. C., M. Al-Daous, S. Sokolov, et al. J. Mater. Chem. 12 (2002) 3261–3267
[8] Junejo A., I. A. Abbasi, et al. Water, Air, and Soil Pollution. (2024) 236
[9] Brown J., L. Mercier, and T. J. Pinnavaia. Chem. Commun. (1999) 69–70
[10] Ma T. Y., X. J. Zhang, G. S. Shao, et al. J. Phys. Chem. C 112 (8) (2008) 3090–3096
[11] Zhang X. J., T. Y. Ma, and Z. Y. Yuan. J. Mater. Chem. 18 (2008) 2003–2010
[12] Horiguchi M., and M. Kandatsu. Nature 184 (1959) 901–902
[13] Li H., G. S. Zhu, X. D. Guo, et al. Eur. J. Inorg. Chem. (2006) 4123–4128
[14] Demmer C. S., N. Krogsgaard-Larsen, and L. Bunch. Chem. Rev. 111 (2011) 7981–8006
[15] Bujoli B., S. M. Lane, and G. Nonglaton. Chem. Eur. J. 11 (2005) 1980–1988
[16] Vermeulen L. A., and M. E. Thompson. Nature 358 (1992) 656–658

http://www.doi.org/10.62341/ahly2841

[17] Abutartour A., et al. Microporous and Mesoporous Materials. (2014) 196, 1–7